

# Boosting the Optimization of Lithium Metal Batteries by Molecular Dynamics Simulations: A Perspective

Yawen Sun, Tingzhou Yang, Haoqing Ji,\* Jinqiu Zhou, Zhenkang Wang, Tao Qian,\* and Chenglin Yan\*

The Li metal battery is attracting more and more attention in the field of electric vehicles because of its high theoretical capacity and low electrochemical potential. But its inherent disadvantages including uncontrolled lithium dendrites, high chemical activity, and large volume changes hold back the large-scale application of stable Li metal anodes. Recently, various computational studies have been used to facilitate the rationalization of experimental observed phenomenon. In this review, the progress of molecular dynamics simulations in Li metal batteries is highlighted. Molecular dynamics simulations can predict how selected atoms in different systems of Li metal battery will move over time based on a general model of the physics governing interatomic interactions. The analysis of the transport structure of Li ions, the electrochemical process at electronic, atomic, or molecular level, the Li<sup>+</sup> transport mechanism, and the Li deposition behavior are described in detail. Some suggestions are also made about the further potential of molecular dynamics simulations do in Li metal batteries are also made.

## 1. Introduction


Li-ion battery (LIB) is one of landmark in the energy storage without question, on account of its high energy density and reversibility. However, with the higher request in electric vehicle market, the energy density of LIB cannot meet the demand.<sup>[1]</sup> Therefore, Li metal anode was put forward due to its high specific capacity (3860 mA h g<sup>-1</sup>) and low electrochemical potential (-3.040 V versus standard hydrogen electrode).<sup>[2]</sup> Nevertheless, three main problems must be figured out to expand the application of Li metal battery (LMB) in electric market: 1) uncontrolled Li dendrites growth during charge/discharge process which result in low coulombic efficiency (CE) and safety problems more serious; 2) the chemical and thermodynamic instability of Li metal can cause continuous and irreversible reactions between Li metal and electrolyte so that reducing

the capacity of batteries; 3) large volume changes during circulation process can tend to bring about the fragmentation of solid electrolyte interphase (SEI), exposing the fresh lithium metal inside that the electrolyte will continue to react with lithium metal to consume the electrolyte and the growth of dendrite cannot be effectively inhibited (Figure 1).<sup>[3–6]</sup> Several ways have been put forward to solve these problems,<sup>[7–9]</sup> but the proposed methods to improve the performance of LMBs still face several influence factors: 1) the solvation sheath of Li<sup>+</sup> in liquid electrolyte and the ion conductivity in both gel and solid electrolyte; 2) the formation and components of solid electrolyte interfaces (SEI); (3) the deposition behavior of Li<sup>+</sup> on the surface of anode. A detailed microscopic understanding of island growth mechanism is required to successful solve these

problems. Recently, some advanced characterization methods (scanning electron microscope, cryo-transmission electron microscope and lots of in situ characterization technology such as in situ X-ray diffraction, in situ fourier transform infrared spectroscopy, in situ UV absorption spectroscopy<sup>[10–12]</sup>) and advanced electrochemical measurement (cyclic voltammetry, impedance test, magnification test, exchange current density, and polarization test<sup>[13–16]</sup>) have been employed to figure out the dynamic behavior of different models. However, these characterizations and measurements are only focused on the description of test results in the level of phenomenon, lack of rational explanation. Many applications still need physical theoretical analysis to comprehend their kinetics mechanism, where molecular dynamics simulation can be used to strengthen the insights into the mechanism investigation of LMBs.<sup>[17]</sup>

With the development of computational simulation technique such as Density Functional Theory (DFT) and Finite element simulation, molecular dynamics (MD) is one of the most frequently-used computational simulations in many fields. It is a science of simulating the motions of particles in system which combines with physics, mathematics and chemistry. Therefore, it can help researchers understand properties of assemblies of molecules by calculating the forces under different interaction potentials. Generally speaking, MD simulate can be divided into classic molecular dynamics (CMD) under Newtonian equation, reactive molecular dynamics (RMD) under reaction force field, ab initio molecular dynamics (AIMD) under Schrodinger

Y. Sun, T. Yang, H. Ji, J. Zhou, Z. Wang, T. Qian, C. Yan  
College of Energy  
Key Laboratory of Advanced Carbon Materials and Wearable Energy  
Technologies of Jiangsu Province  
Soochow University  
Suzhou 215006, P. R. China  
E-mail: jhq18@suda.edu.cn; tqian@suda.edu.cn; c.yan@suda.edu.cn

 The ORCID identification number(s) for the author(s) of this article can be found under <https://doi.org/10.1002/aenm.202002373>.

DOI: 10.1002/aenm.202002373

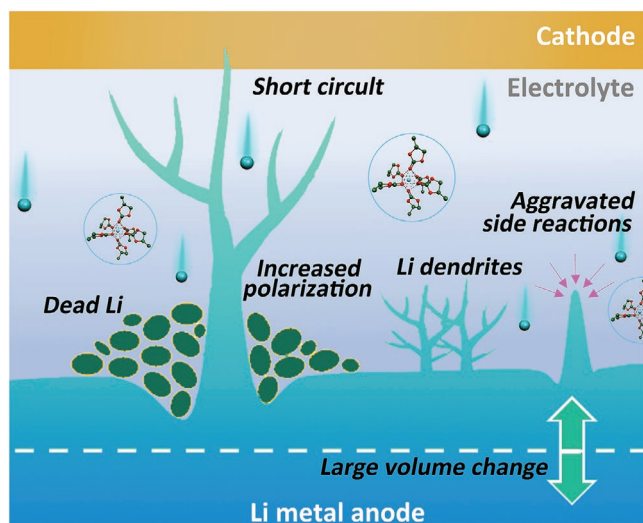


**Figure 1.** The schematic diagram of problems occurred in Li metal battery.

equation and coarse-grained molecular dynamics (CGMD) simulations between all-atom simulation and mesoscopic simulation.

First, in CMD simulations, the basic equation is as follows

$$E_{\text{system}} = E_{\text{vdW}} + E_{\text{Coulomb}} + E_{\text{intramolecular}} \quad (1)$$

where we usually use Lennard-Jones potential to calculate  $E_{\text{vdW}}$

$$E^{LJ} = 4\epsilon \left[ \left( \frac{\sigma}{r} \right)^{12} + \left( \frac{\sigma}{r} \right)^6 \right] \quad (2)$$

With two parameters  $\sigma$  representing diameter and  $\epsilon$  representing well depth. The simplest intramolecular interaction will include bond, angle, dihedral, and improper dihedral. The system is made up of  $N$  interacting atoms or molecules. The atoms are represented by a rigid model which are attracting or repelling by distance without considering electronic structure. The combination of bonded and nonbonded interactions usually provide forces acting on the particles after assigning point charges to each particle.<sup>[18]</sup> This is because the electrons are regarded as ground state without polarization and bond formation and breaking under Born-Oppenheimer approximation. Nowadays, AMBER (Assisted Model Building with Energy Refinement), GROMOS (GRoningen Molecular Simulation), CHARMM (Chemistry HARvard Macromolecular Mechanics) and OPLS-AA (Optimized Potential for Liquid Simulations-All Atom) are four frequently-used force fields in CMD. They have the same function formation but different parameters.<sup>[19]</sup>

In addition, the most widely used reaction force field is ReaxFF (called ReaxFF MD) and it is the bridge between quantum chemistry and classic Newtonian mechanics as the chemical bonds could break or connect freely inside of fixing in the molecular which makes it possible to study the chemical reaction process in large-scale condensed matter. Therefore, reaction force field can deal with chemical reactions compared with CMD and it is more efficient when calculating large systems than AIMD.<sup>[19]</sup> The bond order (BO) concept is the core idea of ReaxFF MD, in which the interaction between atoms is defined as the function of BO and divide into bond,

angle, dihedral angle, conjugate, Coulomb, van der Waals and adjustments

$$E_{\text{system}} = E_{\text{bond}} + E_{\text{lp}} + E_{\text{over}} + E_{\text{under}} + E_{\text{val}} + E_{\text{pen}} + E_{\text{coa}} + E_{\text{C2}} + E_{\text{triple}} + E_{\text{tors}} + E_{\text{conj}} + E_{\text{H-bond}} + E_{\text{vd Waals}} + E_{\text{Coulomb}} \quad (3)$$

Finally, in AIMD simulation, the basic equation is as follows

$$\mathcal{H}(r, R) = -\sum_i \frac{\hbar^2}{2M_i} \Delta_i + \mathcal{H}_e(r, R) \quad (4)$$

where  $\hbar$  represents Plank constant,  $M_i$  represents the mass of given nucleus,  $\Delta_i$  is Laplace operator,  $r$  and  $R$  is the ensemble of all electronic coordinates and all nuclear coordinates respectively. Finite-temperature dynamical trajectories are generated under the forces which can be obtained directly from electronic structure calculations. Thus, AIMD allows chemical bonds breaking and forming too. The AIMD simulations usually consist of  $N$  nuclei and  $N_e$  electrons and consider the Born-Oppenheimer approximation is valid. The dynamics of nuclei can be treated on the ground-state electronic surface classically where the electronic structure method most used is Kohn-Sham formulation.<sup>[20]</sup> CMD relies on semi-empirical effective potentials which is similar to quantum effects, while AIMD is based on the real physical potentials.<sup>[21]</sup> Various properties such as structure, electronic structure, ion solvation structure, ion diffusion, chemical reaction, thermal stability, intermolecular interactions and surface properties can be calculated by MD under different conditions which are called canonical ensemble (NVT), microcanonical ensemble (NVE), isothermal isobaric ensemble (NPT) and isenthalpy isobaric ensemble (NPH) in professional.<sup>[22]</sup>

Beside the all-atom simulations mentioned above, large scale dynamic behavior can be simulated by CGMD and it can reflect more information on the micro level. The effective pairwise forces of CGMD simulations between coarse-grained sites is obtained by averaging the atomistic forces between the corresponding atomic groups from all-atom MD simulations.<sup>[23,24]</sup> Therefore, the CGMD makes up for the shortcomings of all-atom simulations to some extent, and is the “bridge” between all-atom simulation and mesoscopic simulation.

Up to now, some reviews about computational simulations used in cathode materials are mainly focusing on the structure properties, electrochemical behaviors and stability.<sup>[17,22]</sup> Beside these, the theoretical calculations review of other kind of battery-chloride ion battery have been presented to auxiliary screening appropriate materials with outstanding capacities and gravimetric density.<sup>[25]</sup> It is significant to note that a working battery includes cathode, anode and electrolyte. In this review, we summarize the electrochemical process at electronic, atomic or molecular level in the field of Li metal batteries by using MD simulations. Different kinds of multiscale models are discussed based on three aspects: the diffusion and solvated structure of  $\text{Li}^+$  in electrolyte; the formation and  $\text{Li}^+$  diffusion in electrode/electrolyte interface and Li deposition behavior under different conditions (Figure 2). The simulation methods in LMB are summarized to enhance the insights into the optimization of electrolyte formulation, the mechanistic understandings and models for SEI formation, and the behavior of Li depositing.



**Figure 2.** The schematic diagram of the applications of MD in Li metal battery.

The overall purpose is to visualize how the field of LMBs has benefitted from and progressed by the MD simulations.

## 2. Electrolytes

The appropriate electrolyte systems play an important role for Li metal battery design, which serve as function for ion transport. It has been demonstrated that the discovery of appropriate electrolyte systems, such as solid-state, gel and liquid electrolytes in combination with different salt concentration and organic solvents, can inhibit the dendrite formation and improve the stability of Li metal anode, where a myriad of kinetic phenomena occurs in these systems. The presence of positive and negative ions in different electrolyte systems were often accompanied by polarizing solvent molecules and strong local electric fields. In order to throw light on kinetic ion-ion, ion-solvent, ion-polymer interactions, models based molecular simulations were used to predict properties of such systems by investigating bulk properties such as Li ion migrate mechanism and diffusion of charge carriers, which employ results from quantum molecular calculations and atomistic dynamic simulations. Specific attention based on CMD, AIMD, and CGMD is paid to evolve systems dynamically to explore the theoretical understandings and mechanism for these different electrolyte systems.

### 2.1. Liquid Electrolytes

Liquid electrolytes are the most common electrolytes for Li metal batteries, and the solvents must be polar enough to dissociate the Li salt while maintaining electrochemically inert in a wide potential range between 0 and 5 V. These requirements limit the choice of solvents, which are mainly selected from linear and cyclic carbonates. Kumar et al. using CMD simulations analyzed the solvation structure of Li ions in ester electrolyte and found that EC molecules tetrahedrally coordinate with Li<sup>+</sup> ions, forming the Li<sup>+</sup> solvation sheath as shown in **Figure 3a**.<sup>[26]</sup> Some of PF<sub>6</sub><sup>-</sup> ions can enter the inner sphere of the Li<sup>+</sup> solvation sheath. For each electrolyte, the mean-square

displacements (MSD) of Li ions and D<sub>Li<sup>+</sup></sub> values are obtained by the Einstein relation as follows

$$D_{\text{Li}^+} = \frac{\langle \text{MSD} \rangle}{6t} = \frac{\langle |R_{\text{Li}}(t) - R_{\text{Li}}(0)|^2 \rangle}{6t} \quad (5)$$

where  $R_i(t)$  is the position of Li ion at time, and the angle brackets indicate the ensemble average over the MD simulation time. The diffusion coefficient of Li ions in ethylene carbonate (EC) solvent at 330 K was calculated to be  $1.44 \times 10^{-10} \text{ m}^2 \text{ s}^{-1}$ , which is close to the experimental values. The mobility of Li ion is another important dynamic quantity to examine the transport of ions through the solvent, which can be calculated by the drift velocity averaged over all Li ions

$$\mu = \langle V_d \rangle / E \quad (6)$$

where  $E$  is the applied external electric field,  $\mu$  is the ionic mobility and  $V_d$  is the averaged drift velocity. LMB performance is strongly influenced by the diffusion coefficient and mobility of Li ions in different solvent, especially tested in the extreme circumstances, such as extreme temperature systems and low salt concentration systems, depending on the speed at which Li ions transfer across the battery and relating to their solvation structure. The ionic conductivity is also a significant parameter for electrolytes. Ting and colleagues used CGMD simulations on a series of coarse-grained ionomer melt in the presence of an invariable, external electric field. They found that there is a linear response regime between electric field and ion transport when  $E \leq 1 \text{ V}$  because the force between the two ions is much stronger than that of the external field on one ion at this time. The ionic conductivity ( $\sigma$ ) can be calculated as follows

$$\sigma = e \sum \rho |z| \mu \quad (7)$$

where  $e$ ,  $\rho$ ,  $z$ , and  $\mu$  represent the electronic charge, the number density, valence state of the ion and ionic mobility, respectively.<sup>[27,28]</sup> The ionic conductivity of ionic liquid has also been calculated by AIMD simulations to clarify the relationship between ionic conductivity and different fluorinated organic anions of 1-*n*-butyl-3-methylimidazolium salts [BMIM]<sup>+</sup>[Anion]<sup>-</sup>.<sup>[29]</sup> The ionic conductivity is determined by the volume and self-diffusion coefficient of ionic liquids, which is C<sub>4</sub>F<sub>9</sub>SO<sub>3</sub><sup>-</sup> < C<sub>3</sub>F<sub>7</sub>COO<sup>-</sup> < PF<sub>6</sub><sup>-</sup> < CF<sub>3</sub>COO<sup>-</sup> < CF<sub>3</sub>SO<sub>3</sub><sup>-</sup>, corresponding to calculated results. It is clearly shown that MD simulations are an effective way to explore the ionic conductivity of different electrolyte systems.

Li ion solvation and diffusion properties based upon LiPF<sub>6</sub> in EC/PC solvents were further studied by Chaudhari et al. using CMD and AIMD simulations (**Figure 3d**).<sup>[30]</sup> The solvation structure of Li ion in both EC and PC solvent resemble the hydration structure. The results exhibit that first solvation shell is more complex structured in CMD simulation, and the intensity of first peak for radial distribution of carbonyl oxygens around Li<sup>+</sup> is twice above that of in AIMD simulation. Compared to AIMD results, a closer and tighter structuring is observed for the first Li<sup>+</sup> solvation shell, leading to a lower Li<sup>+</sup> diffusion coefficient and a slower exchange of EC/PC molecules around Li<sup>+</sup>. Unlike in glymes and tetraglyme solvents where Li<sup>+</sup> ions are primarily coordinated by only one solvent molecule with consuming a very long time, it is thought that four to five EC/PC molecules directly coordinate with the Li<sup>+</sup>, forming

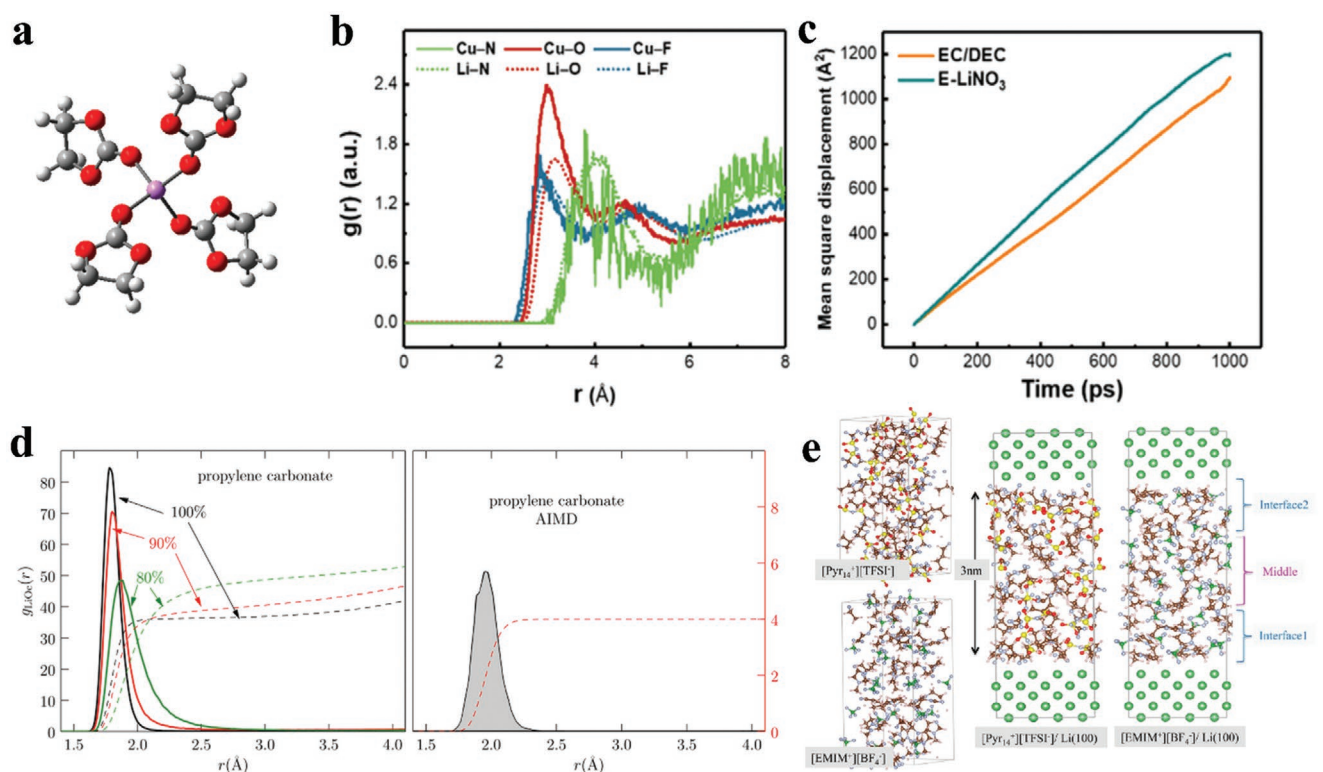


**Figure 3.** a) EC molecules coordinate with  $\text{Li}^+$  ions, forming the  $\text{Li}^+$  solvation sheath. Reproduced with permission.<sup>[26]</sup> Copyright 2016, American Chemical Society. b) Radial distribution functions and c) mean square displacement of Li ions in  $\text{LiNO}_3/\text{EC}/\text{DEC}$  electrolyte. Reproduced with permission.<sup>[41]</sup> Copyright 2018, Wiley-VCH. d) Radial distribution of carbonyl oxygens in PC around  $\text{Li}^+$  using (left) FFMD and (right) AIMD simulations. Reproduced with permission.<sup>[30]</sup> Copyright 2016, American Chemical Society. e) Optimized structures and Interface structural models of bulk IL for  $[\text{pyr}_{14}][\text{TFSI}]$  and  $[\text{EMIM}][\text{BF}_4]$ . Reproduced with permission.<sup>[40]</sup> Copyright 2017, American Chemical Society.

the first  $\text{Li}^+$  solvation shell, which contributes to the  $\text{Li}^+$  transport significantly. With the decreasing of partial charges, the first  $\text{Li}^+$  solvation shell becomes looseness of structure, where the CMD results and AIMD results have no difference. Therefore, the CMD results lead to a tighter structure in the first solvated shell compared with the AIMD studies, and the authors recommended a scaling factor of 80% partial charge on EC and 90% on PC. To further investigate the role of the second solvation shell, systems of  $\text{LiPF}_6$  with EC and additional DEC or dimethyl carbonate (DMC) electrolyte were simulated.<sup>[31,32]</sup> The second solvation shell might be an EC/PC-depleted domain, and the interactions between additional molecules and ion become weaker. Lim et al. use CMD simulations to clearly demonstrate that the increased energy and extra time are needed during the chemical exchange processes in the case of  $\text{LiPF}_6/\text{DEC}$  or  $\text{LiPF}_6/\text{DMC}$  electrolytes.<sup>[33]</sup> The other Li ion solvated structure in different solutions, such as 1,2-dimethoxyethane (DME) and PC have also been simulated by MD.<sup>[34]</sup>

Briefly, solvated structures of Li ions in LMB have been of great importance to understand the dynamics and structure of electrolytes, and different MD simulations can be used to study solvation structure around the  $\text{Li}^+$  ion and the dynamical properties of solvents in the Li ion solvation sheath for various solvent systems. Some of works show that the  $\text{Li}^+$  ions are inclined to solvated by linear carbonate, but some others exhibit that they preferentially solvated by cyclic carbonate. It is still hard and imprecise to specify the properties of the first solvation shell by MD simulations.

Apart from the additives and solvents, the choice of Li salt is clearly important for the electrolyte of Li metal batteries, which is based on large molecular anions with delocalized charges. According to the Barthel et al.'s report,<sup>[35]</sup> the strength of the cation-anion is the most important part for the appropriate Li salts, which directly promotes to the high ionic conductivity of the electrolyte. Jónsson et al. sorted out 53 anions involved in cation-anion interaction,<sup>[36]</sup> including traditional weakly coordinating anions ( $\text{PF}_6^-$ ,  $\text{BF}_4^-$ ,  $\text{ClO}_4^-$ ,  $\text{AsF}_6^-$ , etc.), simple anions ( $\text{Cl}^-$ ,  $\text{F}^-$ ,  $\text{Br}^-$ ,  $\text{NO}_3^-$ ,  $\text{HF}_2^-$ , etc.), imide anions ( $\text{FSI}^-$ ,  $\text{TFSI}^-$ ,  $\text{PFSI}^-$ , etc.), boron based anions ( $\text{B}(\text{C}_6\text{F}_4\text{O}_2)_2^-$ , etc.), phosphorous based anions ( $\text{PF}_3(\text{C}_2\text{F}_5)_3^-$ , etc.), and heterocyclic ring-based anions ( $\text{N}_5^-$ ,  $\text{N}_5\text{C}_2^-$ ,  $\text{N}_5\text{C}_8^-$ , etc.) toward Li ions by DFT and a high level AIMD composite method. With the help of many-body polarizable force fields, MD simulations were performed by Kumar et al. to exhibit that the composition of the interfacial layer near graphite by  $\text{LiPF}_6$  based electrolyte depends on the electrode potential.<sup>[26]</sup> The solvation structures of  $\text{Li}^+$  ions and  $\text{PF}_6^-$  ions in different carbonate-based solvents were further studied by AIMD and ReaxFF MD.<sup>[33]</sup>

In the traditional scenario of  $\text{Li}^+$  depletion model with low concentrated electrolytes near 1 M, the majority of Li ions move with its solvation sheath, and less moves from exchange of solvent molecules. The increased salt concentration can increase the threshold current density and thus inhibit the formation of dendrites. The presence of high concentrated TFSI<sup>-</sup>/TFSI<sup>-</sup> anion in electrolyte can suppress the reductive decomposition

of solvents, where the anions can be reduced prior to solvents in the electrolyte.<sup>[37–39]</sup> According to this interpretation, a new class of electrolyte for fast charging battery with a superconcentrated lithium bis(trifluoromethanesulfonyl)amide (LiTFSA) and acetonitrile (AN) electrolyte has been reported. Li metal anode cannot directly work in a dilute LiTFSA/AN electrolyte due to the poor reductive stability of AN, which can be easily reduced by Li metal to generate the highly toxic free cyanide. This is clearly demonstrated by AIMD simulation that the energy levels of TFSA<sup>−</sup> anion are much higher than that of free AN or Li<sup>+</sup>-solvating molecules at the lowest end of conduction bands and the LUMO is located at AN molecules. As for the 4.2 M LiTFSA/AN electrolyte, the ions pairs are formed by the interacting between TFSA<sup>−</sup> anions and multiple Li<sup>+</sup> cations. The localized LUMOs of TFSA<sup>−</sup> anion demonstrate that the TFSA<sup>−</sup> anions are mainly reduced to form a TFSA-derived surface film, and the anions can govern the reductive stability partly. On account of charge transfer from Li<sup>+</sup> to the TFSI<sup>−</sup>, room temperature AIMD simulation study by Yildirim et al clearly demonstrates that S–N and C–S bond cleavage can initiate the rapid decomposition of the TFSI<sup>−</sup> anions.<sup>[38,40]</sup> A high temperature is required for the decomposition reactions of BF<sub>4</sub><sup>−</sup> anion and cations. The fragments generated by the [pyr<sub>14</sub>] [TFSI<sup>−</sup>] decomposition can be found as SEI components, and promote the charge transfer of LMB (Figure 3e).

Recently, some works show that the adding of additives can improve the ionic mobility, which is beneficial for Li metal battery at large current density.<sup>[41,42]</sup> The additives in the electrolyte, even at ppm levels, can polymerize, adsorb, and decompose on the surface of Li metal anode, which can improve the physicochemical properties of SEI layer and homogenize the current distribution to inhibit the Li dendrite formation. Classic additives, such as various surfactants, organic aromatic compounds, 2-methylfuran, vinylene carbonate, and gaseous molecules, are investigated in the field of LMB. In LiNO<sub>3</sub>/CuF<sub>2</sub>/EC/DEC (DEC is diethyl carbonate) electrolyte system, the MD simulations shows that due to the higher charge, the interaction between NO<sub>3</sub><sup>−</sup> and Cu<sup>2+</sup> is stronger than that between NO<sub>3</sub><sup>−</sup> and Li<sup>+</sup> (Figure 3b,c). The Li<sup>+</sup> diffusion coefficient in LiNO<sub>3</sub> based electrolyte ( $1.12 \times 10^{-11} \text{ m}^2 \text{ s}^{-1}$ ) is larger than that of EC/DEC electrolyte ( $9.94 \times 10^{-12} \text{ m}^2 \text{ s}^{-1}$ ). Moreover, Li et al<sup>[43]</sup> use MD simulations to investigate the structural and transport properties after adding AN and EC in ionic liquid electrolytes. The adding of AN and EC additives can lead to the partial displacement of Ntf<sub>2</sub> anions from first solvent shell and shift the Li–Ntf<sub>2</sub> coordination from bidentate to monodentate. The adding of additives can reduce the Li–Ntf<sub>2</sub> residence times and increase the ion mobility, further promoting the contribution from structural diffusion of the Li<sup>+</sup> cations. Given the above, using MD simulations may play a more important role in understanding the influence of organic solvents on Li<sup>+</sup> solvation and ion transport properties.

## 2.2. Gel Electrolytes

As the alternative of liquid electrolyte, the gel electrolytes have been shown to effectively inhibit the growth of Li dendrites and exhibit significantly stronger adhesion to Li surfaces. However,

the poor kinetic properties caused by the high interfacial resistance and low ion conductivity at room temperature still obstruct the development of gel electrolyte system. In addition, the poor mechanical properties, low ionic conductivity, and a low Coulombic efficiency after introducing gel electrolyte can lead to battery performance decay. Due to the complexity of the ingredients including liquid electrolytes and polymers, it is very difficult to create required models accurately for MD simulations. Zhou's work used CMD simulations to demonstrate that the selected molecules are concentrating near the PEI based matrix rather than distributing randomly in PEO based matrix.<sup>[44]</sup> Luo et. al studied the distribution of metal ions in different gel electrolyte system to understand the enhancement mechanism of ionic conductivity and migration number by CMD simulations, which caused by the strong affinity.<sup>[45]</sup> Li et al.<sup>[46,47]</sup> characterized the interaction between ions and PVDF according to radial distribution functions (RDF) and Li<sup>+</sup> diffusivity by mean square displacement (MSD) function. These reported works based on MD simulations only focused on distribution and diffusion coefficient of Li ions.

To best of our knowledge, the novel gel electrolytes with excellent mechanical strength, high ionic conductivity, and good contact/adhesion are as important as its function of inhibiting the formation of Li dendrites. It is very interesting to use MD simulations to explore Li<sup>+</sup> transport mechanism in different gel electrolyte systems. Besides, by-products during cross-linking reactions are highly reactive with Li metal, increasing the resistance and degrading the Li metal battery performance. MD simulations can be used to model the various processes at the cross-linking reactions or the electrode-electrolyte surface, for instance, SEI formation and electrolyte degradation. To apply the MD simulation in the field of gel electrolytes will have bright prospects.

## 2.3. Solid Electrolytes

The solid electrolyte is one of the promising ways to boost the safe and durable performance of Li metal batteries. However, the development is plagued by the contact issues occurring at solid-solid interfaces. It is essential to have a deep understanding of these mechanisms by both theoretical and experimental study. The solid electrolytes mainly fall into two categories: solid polymer electrolytes and inorganic ceramic electrolytes. For solid polymer electrolytes, the Li salts was blended with polymers, which usually exhibit a mediocre elastic modulus. The ionic conductivity of solid polymer electrolytes is usually several orders of magnitude lower than that of liquid electrolytes.<sup>[48]</sup> Compared with the ceramics, the flexible solid polymer electrolytes exhibit a relatively superior interfacial contact with the electrodes. Amorphous linear and branched poly(ethylene oxide) (PEO) and polyethers doped with Li salts such as LiTFSI, LiCl, LiBF<sub>4</sub>, LiCF<sub>3</sub>SO<sub>3</sub>, and LiI are analyzed by CMD simulations.<sup>[49–53]</sup> Xue et al. studied the diffusion of Li<sup>+</sup> in both amorphous and crystalline PEO/LiCF<sub>3</sub>SO<sub>3</sub> electrolyte by AIMD, which explains that the ionic conductivity of amorphous is higher than crystalline (Figure 4a).<sup>[54]</sup> Lu et al. use the CGMD to describe how ionic aggregation impacts on charge and ion transport and polymer-chain driven mechanisms in PEO-based

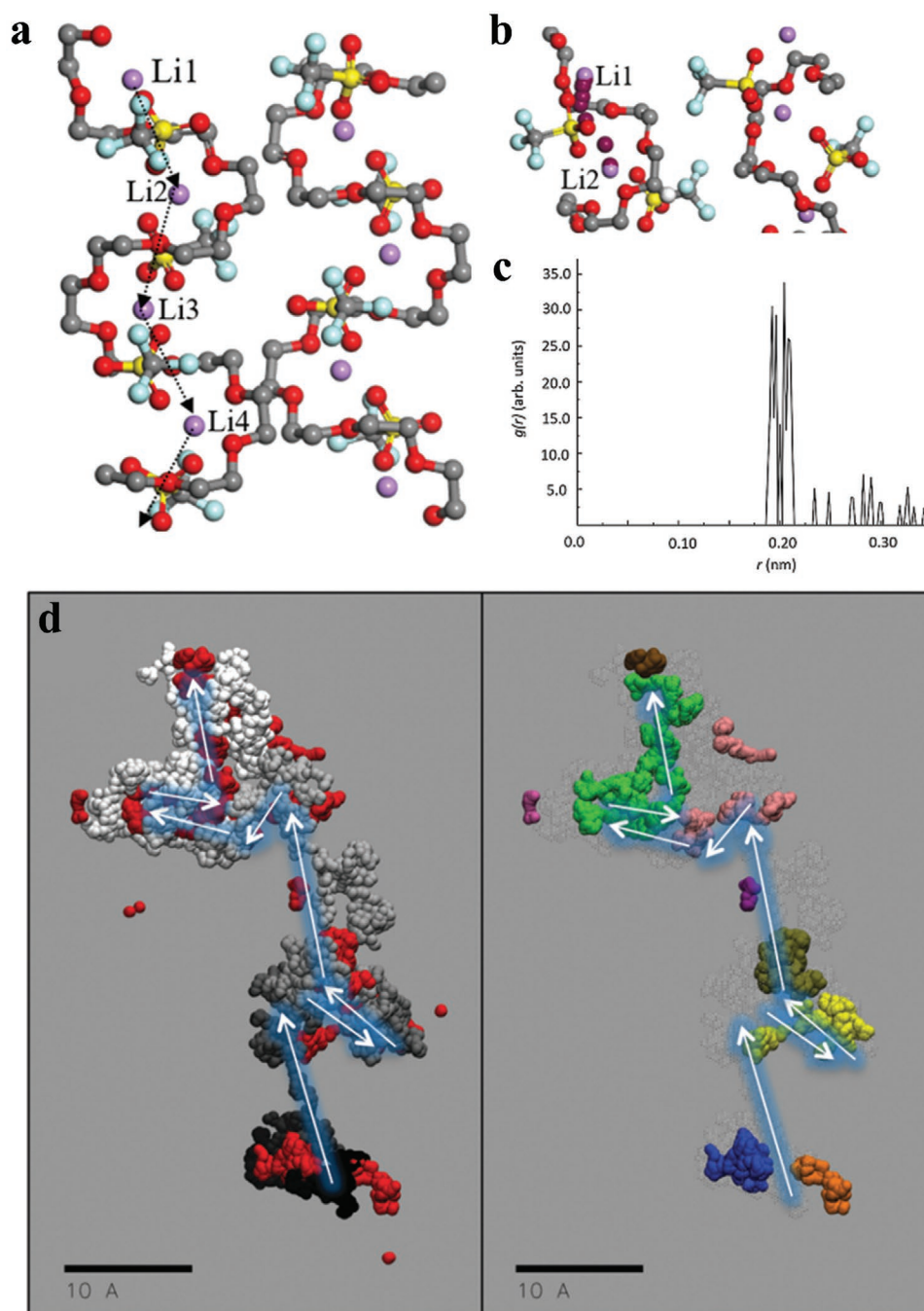


**Figure 4.** a) The initial and final configurations for diffusion of the Li ions in amorphous  $\text{PEO}_3/\text{LiCF}_3\text{SO}_3$ . Reproduced with permission.<sup>[54]</sup> Copyright 2017, Elsevier. b) Optimized pathway of Li1. c) Radius distribution function for the Li–O distances. d) The cation and anion trajectory over 0.5 ns. Reproduced with permission.<sup>[55]</sup> Copyright 2016, Royal Society of Chemistry.

ionomers (Figures 4b–d and Figure 5a).<sup>[55]</sup> The results demonstrate that the ionic aggregates can serve as conduction paths for positive charges, and further reveal how local excess cations coordinate with higher order clusters and ion pairs, moving from one center of the chains to another center of the chains. Moreover, the charge transport can facilitate the movement of collective cation, leading to a faster diffusion rate than any other individual ion moving. For amorphous PEO, it is necessary to

perform long time MD simulations to calculate the diffusion coefficient in solid polymer electrolyte system accurately.<sup>[56]</sup> In a sharp contrast, some simple and convenient simulations can precisely determine the result between crystalline PEO-based electrolyte and ceramic nanoparticles (Figure 5b).<sup>[57]</sup> Structure and dynamics inside solid electrolyte can be simulated, and the cations can disturb the helix of PEO and reduce the motions of polymer chain. The Li ions are diffusing along the PEO chains,

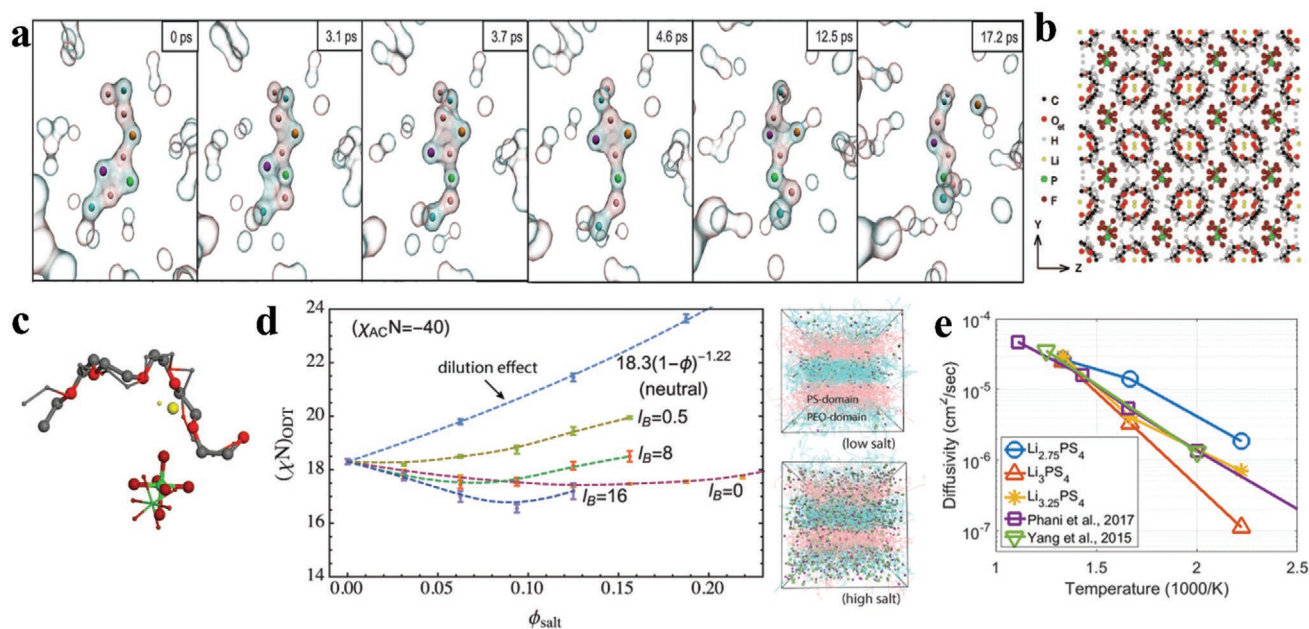


**Figure 5.** a) Snapshots from simulation of ion aggregates conducting charge. Reproduced with permission.<sup>[55]</sup> Copyright 2016, Royal Society of Chemistry. b) The MD simulation box for the crystalline  $\text{LiPF}_6/\text{PEO}_6$  system. Reproduced with permission.<sup>[57]</sup> Copyright 2005, Royal Society of Chemistry. c) The “folded” asymmetric unit of  $\text{LiPF}_6/\text{PEO}_6$  resulting from MD simulation and the ND-determined asymmetric unit<sup>5</sup>. d) Shift in  $(\chi_{AB}^N)_{\text{ODT}}$  as a function of salt concentration. Reproduced with permission.<sup>[58]</sup> Copyright 2016, American Chemical Society. e) Tracer diffusivity from the current MD simulations. Reproduced with permission.<sup>[64]</sup> Copyright 2018, American Chemical Society.

and anions can help cations to transfer from one PEO chain to another. Moreover, the ordering transition of block copolymers with charges were investigated by the CGMD simulation of diblock PEO-PS copolymers doped with LiTFSI (Figure 5c,d).<sup>[58]</sup> A coarsegrained simulation model was introduced to treat electrostatic interactions explicitly and distinguish between the solvent dilution effect and ion association effect, which are two competing effects, leading to the change of the order-disorder transition temperature (ODT). The result shows that solvent dilution, association of Li-like cations with PEO-like blocks, the strength of Coulomb interactions, and selective solvation due to Born solvation can impact the ordering transition of ionic polymeric systems. The simulation of nonlinear dielectric screening, ion clustering, and ion polarizability require a model with reliable polarizable force fields and hard-core potentials.

Compared with solid polymer electrolytes, inorganic ceramics exhibit satisfactory mechanical properties and high ionic conductivity. Most of inorganic ceramics possess high elastic modulus to prevent the formation of Li dendrites.  $\text{Li}_{10}\text{GeP}_2\text{S}_{12}$ ,  $\text{Li}_{9.54}\text{Si}_{1.74}\text{P}_{1.44}\text{S}_{11.7}\text{Cl}_{0.3}$ , and some inorganic ceramics have a high ionic conductivity approaching or even exceeding that of liquid electrolytes.<sup>[48]</sup> However, high-modulus materials are leading to a poor interfacial conductance between the electrode and inorganic ceramics. An ionblocking layer is generated in the interface due to the redox reactions, severely affecting the cell kinetics. The corresponding MD simulations based on inorganic ceramic system, such as  $\text{Li}_9\text{S}_3\text{N}$  and  $\text{Li}_{10}\text{GeP}_2\text{S}_{12}$ , are focused on the diffusion mechanisms and  $\text{Li}^+$  ion conductivity.<sup>[59–61]</sup> In these works, MD simulations were only used to predict conductivities and migration energies throughout the crystal structure at different inorganic

ceramics, which need to support the experimental results. Detailed analysis of AIMD simulations were used to explore the conductivity change caused by isovalent cation substitution and evaluate lattice parameter changes on transport properties, further demonstrating that Li conductivity is connected with lattice parameters. The shrinking size of transport channels will slow down the Li diffusion. Furthermore, the  $\text{Li}_{10}\text{GeP}_2\text{S}_{12}$ -type conductors with high ionic conductivity was simulated by Oh et al, and AIMD simulations was used to identify that major defects can facilitate  $\text{Li}^+$  diffusion and offer a more flattened site energy landscape along the c-channel.<sup>[62]</sup> The results further demonstrated that the major defects in inorganic ceramics significantly alter the diffusion process, which can flatten the site energy landscape and enhance the charge carrier concentration, leading to a fast lithium diffusion. Similarly, Mo and coworkers put down the fast ionic conduction to the facile Li diffusion along the c-axis based on AIMD simulations.<sup>[63]</sup> Klerk and colleagues researched the Li-ion diffusion in  $\text{Li}_3\text{PS}_4$  based on thorough analysis of MD simulations, which indicated that Li-ion diffusivity can be increased by the acceleration of the rate-limiting jump process (Figure 4e).<sup>[64]</sup> To the best of our knowledge, MD simulations can be used to demonstrate how the designed approaches help the Li ion diffusion in inorganic ceramic electrolytes, and how this provides direction to design new and improved inorganic ceramic electrolytes.

### 3. Electrode/Electrolyte Interface

A surface layer can be formed between Li metal anode and electrolyte during the first cycle because the Li metal can react with

most organic electrolytes. Good morphology and structure of SEI can inhibit lithium dendrites growing and make for excellent performance of LMBs while the growth of dendrites will be uncontrolled with poor structural SEI. There is quite a success with constructing artificial interfaces to deal with inferior SEI. However, it is difficult for us to understand the formation mechanism, electrochemical reaction and Li ions transport between electrode/electrolyte interface due to it is too complex to observation clearly and real-time. In order to illuminating the kinetic of SEI formation and ion transport, models based on MD simulations were used to help us realizing the basic progresses on the behavior which successfully solved the issues mentioned above.

### 3.1. Initial Solid Electrolyte Interphase (SEI)

Due to the high negative electrochemical potential of  $\text{Li}^+$ /Li, most organic electrolytes can be reduced to form the passivating SEI layers on the anode surface.<sup>[65–67]</sup> The stability of SEI has an immediate impact on Li stripping and plating progresses and electrochemistry performance of Li metal battery, which can address the challenges of lithium metal. An ideal SEI should be uniformly covered on the surface of Li metal with a relatively thin and compact structure, which has a high elastic strength and excellent ionic conductivity.

Balbuena and coworkers used reactive molecular dynamics to simulate the formation of SEI with zero bias potential and 1 M Li salt in different polar solvents. The surface of Li metal anode became dissolved as soon as contacting with electrolytes and the dissolved part which is called porous phase included nest phase and disperse phase. In the nest phase, the Li atoms connected with themselves and dense phase and formed an amorphous region which can provide channels for the nonreacted electrolytes. On the contrary, the Li atoms concatenated with residual decomposed production and unreacted species instead of themselves in the disperse phase. To sum up, the Li atoms with higher oxidation in disperse phase is where the SEI nucleates (**Figure 6a**).<sup>[68]</sup> The same simulation results can be seen in 1 M LiFSI in DME with a Cu electrode by increasing voltage.<sup>[69]</sup> It is in keeping with other researchers' result that the SEI in carbonate-based electrolytes usually contain outer and inner layers. On the one hand, the inner layer often consists of inorganic substance, such as  $\text{Li}_2\text{O}$ , LiF,  $\text{Li}_3\text{N}$ , and  $\text{Li}_2\text{CO}_3$ . On the other hand, the outer layer is considered to be made up of alkyl dicarbonate matters, such as dilithium ethylene dicarbonate ( $\text{Li}_2\text{EDC}$ ) and dilithium butylene decarbonate ( $\text{Li}_2\text{BDC}$ ).<sup>[70,71]</sup> Surface structure as well as the components of SEI are no doubt important for the LMBs because the surfaces are not expected to be stable in both liquid and polymer electrolytes.

AIMD was used to study the different the components of SEI layer. Russo and coworkers simulated the initial stage of SEI between Li metal anode and *N*-Methyl-*N*-Propyl-Pyrrolidinium-Bis(Fluorosulfonyl)Imide ionic liquid ( $[\text{C}_3\text{mPy}^+][\text{FSI}^-]$ ). First, the ion pairs of  $\text{C}_3\text{mPy}^+$  and  $\text{FSI}^-$  were placed on the surface of Li metal (001) and found  $\text{C}_3\text{mPy}^+$  have a tendency to move away from the surface, while  $\text{FSI}^-$  anions exhibit strong combination with lithium atoms. Then after 72, 126, 478, and 543 fs, the LiF,

$\text{Li}_2\text{F}$ , LiO,  $\text{Li}_2\text{O}$  molecules were generated in order respectively. At the time of 694 fs,  $\text{FSI}^-$  anions were consumed mostly and invisible (**Figure 6b–g**).<sup>[72,73]</sup>

The migration and diffusion of Li-ion is the important character of SEI in LMBs, so atom-level understanding of ion diffusion among SEI ( $D_{\text{SEI}}$ ) is instructive to design SEI. Seung et al. reported their results about Li-ion diffusion at the interface between the surface of lithium metal and  $[\text{Pyr}_{14}][\text{TFSI}]$  ionic liquid. They considered two systems: one is a small system for running longer time with 83 Li and 2  $[\text{TFSI}]$ . Another is a large system which may be more accurate with 164 Li and 4  $[\text{TFSI}]$ . After analyzing the trajectory of lithium ion, they owing the  $D_{\text{SEI}}$  to the vacancy-mediated diffusion mechanism. It is usually that F ion in the SEI may coordinate with 3 or 4 Li atoms while O ion may typically match with 4–6 Li atoms. So, for instance, a  $\text{Li}_4\text{O}$  group has two vacancies to accept Li atoms and there is a chance for Li atoms from other  $\text{Li}_n\text{X}$  group ( $\text{X} = \text{S}, \text{F}, \text{N}, \text{C}$ , and O) to jump to these vacancies during thermal vibrations. Resulting new vacancies in the other  $\text{Li}_n\text{X}$  group which will be filled by else Li atoms.<sup>[74]</sup> Hooper and his partners employed MD to simulate model SEIs comprised of  $\text{Li}_2\text{EDC}$  and  $\text{Li}_2\text{BDC}$  in a wide temperature range. Under 120 °C, the SEI model revealed single ion conductor behavior and the ordered materials had higher conductivity than disordered analogues.<sup>[75]</sup>

Besides the solid-liquid interface (Li metal-liquid electrolyte solution), the solid-solid interface (Li metal-solid electrolyte) also be researched about the ion transfer. Recently, more and more solid electrolytes with high ion conductivity have been developed for all-solid-state Li metal batteries to solve the dendrites and safety problems,  $\text{LiBH}_4$  is one of it. The calculated results showed that there is a double-layer capacitance at the interface and the coordination between H and Li atoms plays a significant role in Li transfer coupling with electron transfer. The ion transmission mechanism is activated by a lithium ion moving to a metastable site and then leaving an intrinsic vacancy to be occupied by other ions.<sup>[76]</sup> The initial SEI is too significant to the performance of LMBs, and flexible use of MD simulations can help us understand the formation and the  $\text{Li}^+$  transmission mechanism of SEI clearly.

### 3.2. Artificial Interface

The in-situ formation of SEI layer is too complicated and uncontrollable. To avoid the inhomogeneity and fragility of SEI, a series of strategies have been put forward to build a robust layer, which provide another feasibility to modify SEI films in Li metal batteries. Of particular attention is that the achievements rely strongly on the metal ion-conductivity of such ideal SEI layer. Classical MD simulations can be used to observe the ion transport behavior both in SEI and artificial SEI visibly. Recently, Bao and colleagues put forward a dynamic single-ion-conductive network (DSN) where 1*H*,1*H*,11*H*,11*H*-perfluoro-3,6,9-trioxoundecane-1,11-diol (FTEG) were the inert ligands and  $\text{Al}(\text{OR})_4^-$  ( $\text{R} = \text{FTEG}$ ) anions were chosen as the dynamic crosslinking centers as artificial SEI and simulated the transport of Li ions in it. At first, 64 Li atoms, 128 FTEG chains, and 64 Al centers were distributed uniformly in the computational box. After simulating the system in the NPT ensemble



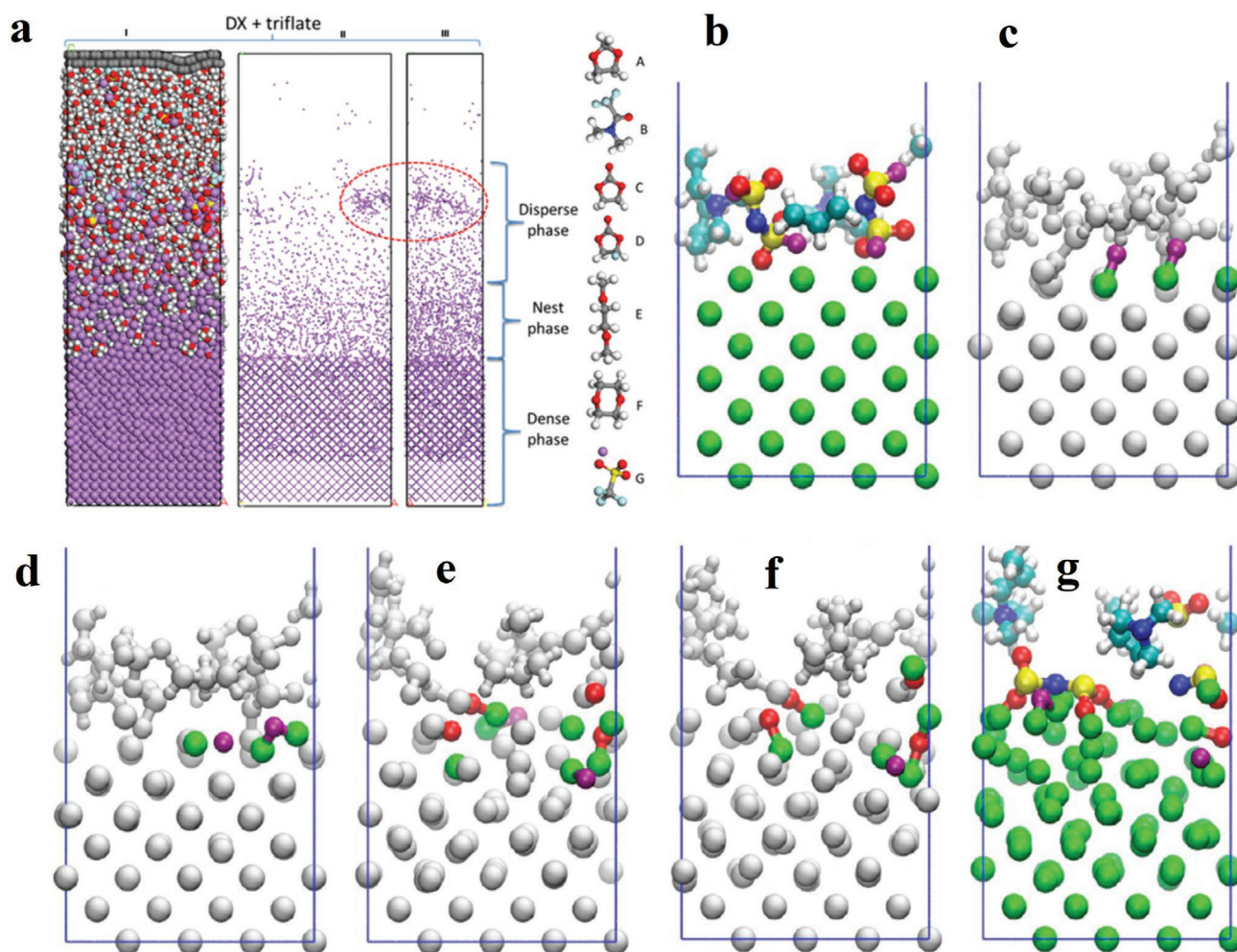


**Figure 6.** a) I) Front-side view of the cell showing all the atoms. II) Front-side view of the cell showing only lithium atoms, while the other atoms are hidden. III) Side view of the cell showing only lithium atoms at 2 ns of simulation with 1 M triflate in 1,4-dioxane. The color scheme used is as follows: Li: purple, O: red, C: gray, H: white, F: cyan, and S: yellow. Reproduced with permission.<sup>[68]</sup> Copyright 2018, American Chemical Society. Snapshots of the simulation trajectory at b) 0 fs, c) 72 fs, d) 126 fs, e) 478 fs, f) 543 fs, and g) final frame (694 fs), the formation of the LiF, Li<sub>2</sub>F, LiO, and Li<sub>2</sub>O species in (b–e) have been highlighted. Color code: Li in green, C in cyan, N in blue, O in red, S in yellow, and F in purple. Reproduced with permission.<sup>[72]</sup> Copyright 2012, American Chemical Society.

for 50 ns whatever the electric field exist or not, what is noteworthy is that that the radial distribution function (RDF) of Li-Al had two peaks which represents DSN may have two Li ion solvation structures. Combining with <sup>7</sup>Li-NMR and <sup>19</sup>F-NMR, they identified the conclusion and reported the Li ion transport mechanism in DSN. First, the pulsatile Li ions are uniting with lower Al centers where the Li-Al distance is 0.32 nm to form Complex 1. Then the pulsatile Li ions move to suspend between Al centers which make the distance of Li-Al increasing to 0.42 nm. Finally, the Li<sup>+</sup> shift to coordinate with upper Al centers to form Complex 2. What is more, the Li<sup>+</sup> can move back and reunite with lower Al centers without extra transition state barrier (Figure 7a–c).<sup>[77]</sup>

The AIMD also can be used to design and filtrate artificial SEI without tedious experiments. Akbulut and coworkers simulated the reactivity between Li<sub>3</sub>N and Li<sub>7</sub>P<sub>3</sub>S<sub>11</sub> solid electrolyte within 1.2 ps and found both of them do not degrade in contact with each other. Then they used Li<sub>3</sub>N as artificial SEI coating

on the surface of Li metal anode and achieved excellent performance.<sup>[78]</sup> For a deeper understanding about the physical origin of upgrading Li ion transference number, Cui and coworkers used MD simulations on polyvinylene carbonate (PVCA)-Li<sub>7</sub>La<sub>3</sub>Zr<sub>2</sub>O<sub>12</sub> (LLZO)-EC/DMC-LiPF<sub>6</sub> system and found both of the diffusion coefficient of Li<sup>+</sup> and PF<sub>6</sub><sup>+</sup> increased with the temperature. Whereas, in this system, the diffusion coefficient of Li<sup>+</sup> was higher than PF<sub>6</sub><sup>+</sup>.<sup>[79]</sup>

#### 4. Li Deposition Behavior

Similar to other alkali metal, Li metal tends to deposit in the dendritic structure, which is known as the fundamental challenges, resulting in low Coulombic efficiency, short-circuiting and thus short lifetime of Li metal batteries. To achieve successful Li metal anodes, we need to obtain a deep understanding of Li deposition behavior.<sup>[80]</sup> Both internal and external

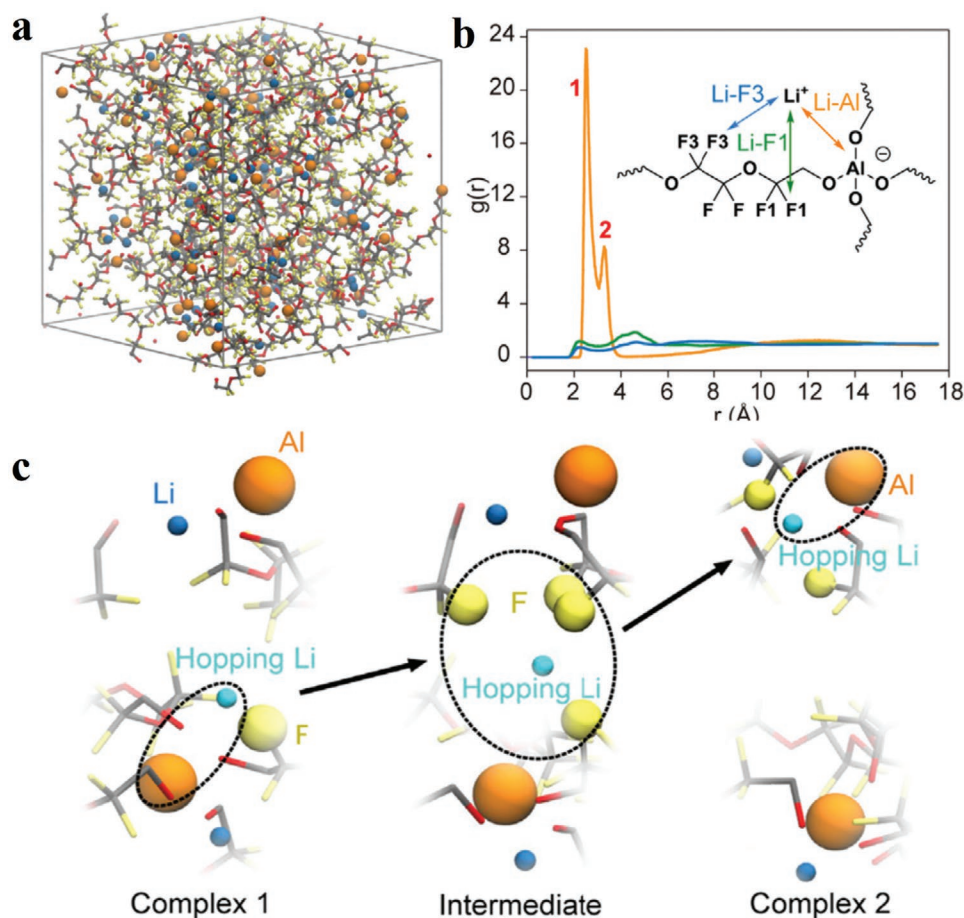


**Figure 7.** a) Optimized structures of the equilibrated DSN systems. Color code: Li<sup>+</sup> ions, blue; Al centers, orange; F atoms, yellow; C atoms, gray; O atoms, red. For clarity, all H atoms are omitted and FTEG chains are shown in stick format. b) Radial distribution functions at equilibrium. Orange, Li-Al; olive, Li-F1; blue, Li-F3. c) Li<sup>+</sup> ion transport pathway. The hopping Li<sup>+</sup> ion is shown in light blue while irrelevant Li<sup>+</sup> ions are dark blue. F atoms within 3 Å of the hopping Li are emphasized with yellow spheres. For clarity, FTEG chains are faded. Reproduced with permission.<sup>[77]</sup> Copyright 2019, Elsevier.

factors can affect the behavior of Li deposition. The external elements usually include temperature, pressure, and fold and the internal elements are containing current density, electrolyte components, the surface properties and morphology of electrode.

It is comprehensible that dendrites growth as the current dendrite continuum modeling frameworks, but it involves simplifying assumption that may miss capturing some atomic scale essentials. MD simulations can be used to analyze the formation of lithium dendrites. In recent work, researchers have found that the growth of dendrites will be destroyed when applying the gradient of temperature during electrodeposition.<sup>[81]</sup> Hoffmann and co-workers simulated the behavior of Li dendrites at the temperature ranging from 317 to 357 K under NVT condition by ReaxFF MD and found the Li dendrites collapsed quickly at the beginning, then formed 3–5 atoms thick layer after 200 ps in most case.<sup>[82]</sup> Therefore, temperature is not harmful to lithium metal batteries as commonly believed, on the contrary, the right temperature can prevent the growth of lithium dendrites. It was observed that the dendrites growing quickly as soon as the solvated Li contacted the surface of anode and the rate maintained until the

moments before the short circuit with the high and sharp dendrites. Nevertheless, the growth is uniform and slow with non-uniform negative charge on the surface. So the distribution of charges, and especially, the concentration of charge on the surface of anode in particular spots such as SEI cracks, determines the dendrites growth (Figure 8).<sup>[83]</sup> It is generally speaking that the dendrites problem will be aggravated under high current density. But Koratkar and coworkers reported a self-heating-induced healing of Li dendrites phenomenon that there is a self-healing of dendrites when the current density raised above 9 mA cm<sup>-2</sup>, which triggers a large area of surface Li migration by MD simulations. Thus the lithium dendrites will be healed and the surface of Li metal will be smooth under the repeated high current density.<sup>[84]</sup>

A lithiophilic matrix can reduce the energy barrier of Li nucleation, balance the electric flux and strengthen the combination between Li atoms and substance.<sup>[85,86]</sup> Qian and coworkers reported an electrolyte additive: tetrachloro-1,4-benzoquinone (TCBQ) in Li metal batteries and found its decomposition product (Li<sub>2</sub>TCBQ) in SEI has high lithiophilicity by classic MD. In detail, a system was established by stacking Li<sup>+</sup> on to the surface of Li<sub>2</sub>TCBQ with the comparison of LiF and

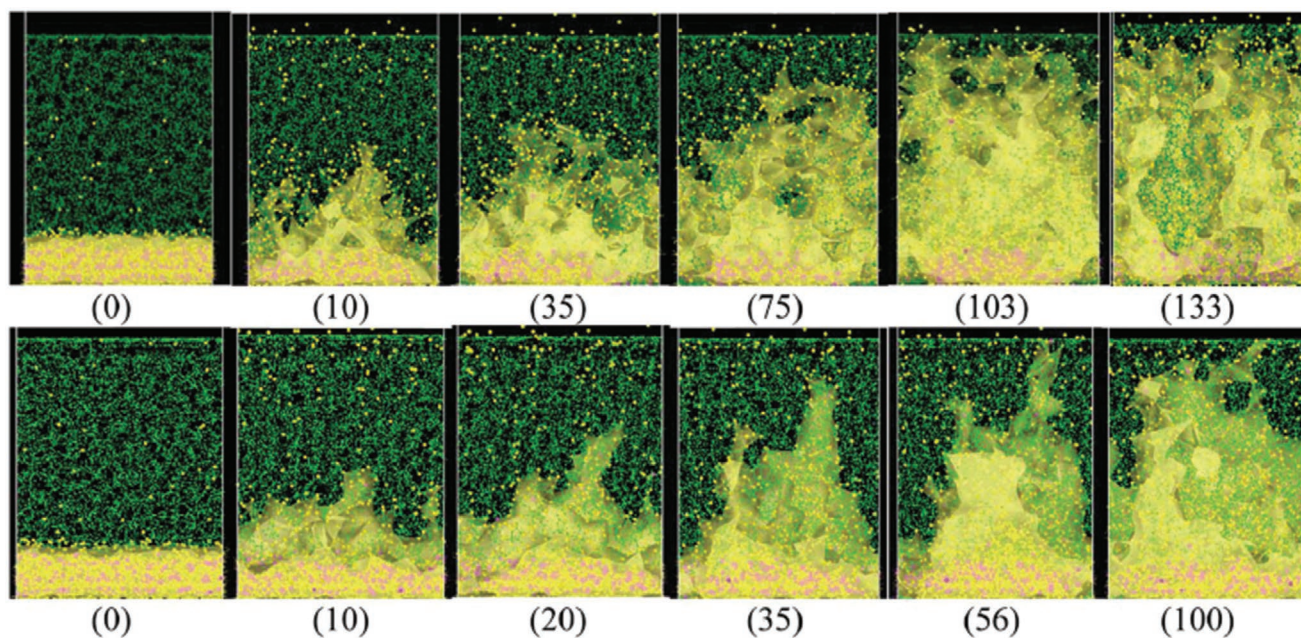


**Figure 8.** The growth of Li dendrites with different charge of atoms on the surface about  $-1e$  (top) and  $-0.54e$  (bottom) during time increasing. Reproduced with permission.<sup>[83]</sup> Copyright 2018, Royal Society of Chemistry.

$\text{Li}_2\text{CO}_3$  surfaces which are the most common components in SEI layer. From the simulated picture we can see that Li ions tend to approach  $\text{Li}_2\text{TCBQ}$  surface because of the affinity of lithium (Figure 9a–c).<sup>[87]</sup> As mentioned above that the SEI in carbonate-based electrolytes usually contain inner and outer layers, a dual-layered is appeared by immersion the Li metal anode into fluoroethylene carbonate solvent with organic components on the top and inorganic components in the bottom by Zhang and coworkers. The organic layer has good flexibility to avoid damage while the inorganic  $\text{Li}_2\text{CO}_3$ -LiF layer guides the orderly nucleation sites and inhibits the formation of lithium dendrites.<sup>[88]</sup> Yamamoto and colleagues used AIMD simulations to calculate the interactions between electrolyte solvents and Li metal surfaces, founding that the oxygen atoms in the ether molecules effortlessly attracted to Li metal surface so the interfacial energies would be smaller than other electrolytes. The assumption of steric effect that higher interfacial energy can retard the formation of dendrites since they would result in larger surface areas can help us know something about Li deposition behavior.<sup>[89]</sup>

Apart from the lithiophilic of SEI surface, an anode which has high affinity of Li ions can also influence the Li deposition behavior. Yan and partners put forward a single-atom iron into nitrogen-doped carbon substance as lithiophilic site to control the nucleation and deposition of lithium metal and was testified by classic MD as well.<sup>[90]</sup> Jump out of the frame, alloy of Li metal and other substances also can be a kind of lithium anode. Wang and coworkers reported a high energy LMBs with Li-Si alloy anode. The structures of amorphous  $\text{Li}_x\text{Si}$  ( $x = 0.33, 1, 2.75, 3.25, 3.75, \text{ and } 4.4$ ) was modeled under ReaxFF force field and Si atoms dispersed uniformly in the Li-Si alloy.  $\text{Li}^+$  transferred to the anode surface under the effect of concentration gradient and electric field, forming alloy by inserting in Si,

when discharging. After that,  $\text{Li}^+$  began plating at the surface of Li-Si alloy around the lithiophilic Si atoms and induced a uniform Li deposition.<sup>[91]</sup> The lithiophilic of both SEI surface and structure can be visualized clearly by different kinds of MD simulations rather than doing complex characterizations to explain the principles, which is convenient and meanwhile credible.

## 5. Conclusions and Outlook

Advances in Li metal battery are extremely urgent for the higher request in electric vehicle market. Lots of solutions have been put forward and analyzed by advanced characterization technologies. But the microscopic changes and mechanism at electronic, atomic or molecular level is remaining incomprehensive. In this review, we present a brief overlook of MD simulations in Li metal battery. On the one hand, the solvated structure of  $\text{Li}^+$  can be visualized clearly by CMD or AIMD including the first solvation shell and the second solvation shell in liquid electrolyte. Since they are based on the disparate equations and force field, the distance between  $\text{Li}^+$  and solvated is different. But the solvated structure is the same which can help us know more about the migration form about  $\text{Li}^+$  in electrolyte. While the polymer-chain driven mechanisms in organic electrolyte and transport along lattice mechanisms in inorganic electrolyte can also be certified by MD simulations. On the other hand, the problems between electrolyte/electrode interface are complicated to understand, however, with the MD simulations, we can know the basic formation of initial SEI or artificial SEI including the components and the migration of  $\text{Li}^+$  in them. Finally, molecular simulation can be used to explain the factors affecting the formation of lithium dendrites which contains

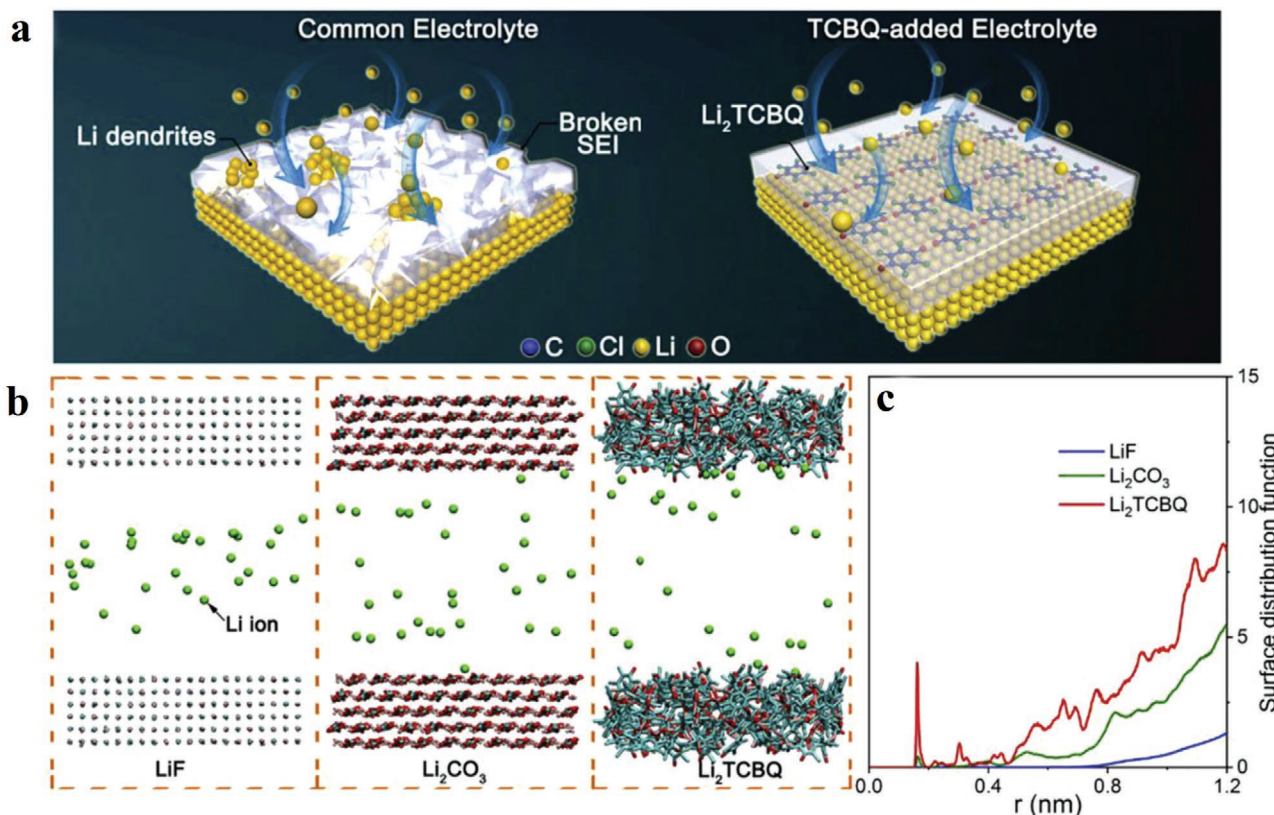


**Figure 9.** a) Schematic diagram of Li deposition in common and TCBQ-added electrolyte. b) MD simulations in LiF,  $\text{Li}_2\text{CO}_3$ , and  $\text{Li}_2\text{TCBQ}$  system with the same electrolyte phase. c) The surface distribution functions (SDF) of Li ions near the three surfaces. Reproduced with permission.<sup>[87]</sup> Copyright 2019, Elsevier.

current density, temperature, electrolyte components and electrode morphology in microcosmic.

As mentioned above, MD simulations can help us learn more about the reactive mechanism and ion transmission route at the electronic, atomic or molecular level in the field of Li metal batteries, which can be divided into CMD, RMD, AIMD and CGMD simulations. Each MD simulation makes a different set of modelling about the system in Li metal batteries and has its own pros and cons (Table 1). If the system has a large number of molecular atoms, CMD simulations will be the first choice to analyze the  $\text{Li}^+$  distribution and solvation structure in electrolytes or on the surface of electrodes. However, the process involving the fracture and formation of

a chemical bond cannot be simulated due to the limitation of the applied force field. AIMD simulation is primarily used to overcome these technical difficulties because of its quantum mechanical properties, which can simulate the decomposition of electrolyte and the formation of SEI.  $\text{Li}^+$  solvation structure and  $\text{Li}^+$  distribution can also be simulated by AIMD simulation, but it can only simulate dozens of atoms, which is the biggest drawback of AIMD simulation. Furthermore, RMD can simulate the breaking and formation of chemical bonds with a large number of atoms. Compared with AIMD, it can simulate thousands or tens of thousands of atoms. Therefore, RMD is often used to simulate dendrite evolution for the different model of Li metal batteries. Finally, CGMD simulation is the “bridge”

**Table 1.** The advantages and disadvantages of different MD simulations in the field of Li metal battery.

Name	Force field	Advantage	Disadvantage	Applications
CMD	classical mechanical force field	can simulate a large number of atoms	cannot simulate the breaking and formation of chemical bonds	$\text{Li}^+$ distribution and solvation structure
AIMD	quantum mechanical force field	can investigate the chemical reaction process; have strong universality and high accuracy;	only can simulate dozens of atoms	$\text{Li}^+$ distribution and solvation structure, the decomposition of electrolyte and the formation of SEI
RMD	reaction force field	can simulate the fracture and formation of chemical bond	the time required is longer than that of CMD	the decomposition of electrolyte and the formation of SEI; dendrite evolution
CGMD	coarse-grained force field	can simulate larger spatial and temporal scales than CMD	low accuracy	the transport of $\text{Li}^+$ , ion aggregation and ion trajectories

between microcosmic simulation and mesoscopic simulation. The coarse-grained force field, which considered a fragment in the molecule as a whole determines that the simulation system can be very large. However, some details, such as local interaction between atoms, cannot be reproduced because of coarse granulation. If you want to look at physical properties that tend to be mesoscopic, such as ion aggregation and ion trajectories, CGMD simulation is a good choice.

Computer simulation can not only provide qualitative description, but also simulate the quantitative results of the structure and properties of materials. With the development of algorithms from simple nonreal molecular systems to complex real molecular systems, MD simulations overcome the shortcomings of monte-carlo method which can only describe the characteristics of the molecular structure at equilibrium state, but can not describe the process of the molecular structure changing with the transformation of the macroscopic physical properties of the system. Currently, the applications of MD simulations in Li metal batteries are mainly focusing on explaining the existing phenomena and helping us to have a deeper understanding of the mechanism. However, few MD simulations have been performed to predict performance or select electrolytes and electrode materials in Li metal batteries before experiments. For future improvement and research directions of Li metal battery systems, integrating MD simulations into the rational design of Li metal batteries is quite promising to be practically applied.

- a) Screening electrochemically stable electrode materials under different voltage by simulating the crystal/molecular structures and their dynamic stabilities during the process of lithiation and delithiation;
- b) Exploring a new type of electrolyte for universal batteries and testing its feasibility by MD simulations, not limited to the existing ester and ether electrolytes;
- c) Understanding the relations between structure and property, and identifying the key parameters related to battery performance;
- d) Predicting the physicochemical properties and conducting experiments under unreachable conditions, such as ultralow or ultrahigh temperature.

In summary, there is still a long way to realize the commercialization of LMBs. Although great achievements have been made in the fundamental research of LMBs, great challenges and opportunities still need to be explored in further research. It is believed that a promising future of LMBs will come by means of MD technology.

## Acknowledgements

Y.W.S. and T.Z.Y. contributed equally to this work. The authors acknowledge the support from the National Natural Science Foundation of China (Grant Nos. 51872193, 21703149, and 51622208) and the Priority Academic Program Development of Jiangsu Higher Education Institutions (PAPD).

## Conflict of Interest

The authors declare no conflict of interest.

## Keywords

electrode/electrolyte interfaces, electrolytes, Li deposition behavior, Li metal batteries, molecular dynamics simulations

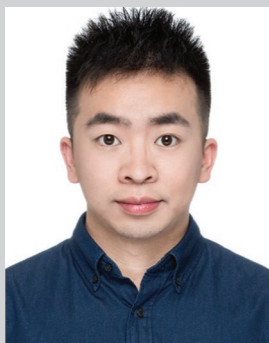
Received: July 22, 2020  
Revised: August 25, 2020  
Published online:

- [1] X. Fan, X. Ji, F. Han, J. Yue, J. Chen, L. Chen, T. Deng, J. Jiang, C. Wang, *Sci. Adv.* **2018**, *4*, 9245.
- [2] F. Qiu, X. Li, H. Deng, Di Wang, X. Mu, P. He, H. Zhou, *Adv. Energy Mater.* **2019**, *9*, 1803372.
- [3] B. Liu, J.-G. Zhang, W. Xu, *Joule* **2018**, *2*, 833.
- [4] R. Cao, W. Xu, D. Lv, J. Xiao, J.-G. Zhang, *Adv. Energy Mater.* **2015**, *5*, 1402273.
- [5] Y. Lu, Z. Tu, L. A. Archer, *Nat. Mater.* **2014**, *13*, 961.
- [6] S.-H. Wang, Y.-X. Yin, T.-T. Zuo, W. Dong, J.-Y. Li, J.-L. Shi, C.-H. Zhang, N.-W. Li, C.-J. Li, Y.-G. Guo, *Adv. Mater.* **2017**, *29*, 1703729.
- [7] X. Chen, M. Shang, J. Niu, *Nano Lett.* **2020**, *20*, 2639.
- [8] F. Zhao, J. Liang, C. Yu, Q. Sun, X. Li, K. Adair, C. Wang, Y. Zhao, S. Zhang, W. Li, S. Deng, R. Li, Y. Huang, H. Huang, L. Zhang, S. Zhao, S. Lu, X. Sun, *Adv. Energy Mater.* **2020**, *10*, 1903422.
- [9] T. Xu, P. Gao, P. Li, K. Xia, N. Han, J. Deng, Y. Li, J. Lu, *Adv. Energy Mater.* **2020**, *10*, 1902343.
- [10] A. M. Tripathi, W.-N. Su, B. J. Hwang, *Chem. Soc. Rev.* **2018**, *47*, 736.
- [11] H. Li, D. Chao, B. Chen, X. Chen, C. Chuah, Y. Tang, Y. Jiao, M. Jaroniec, S.-Z. Qiao, *J. Am. Chem. Soc.* **2020**, *142*, 2012.
- [12] A. J. Leenheer, K. L. Jungjohann, K. R. Zavadil, J. P. Sullivan, C. T. Harris, *ACS Nano* **2015**, *9*, 4379.
- [13] Y. Zhang, Y. Zhong, Z. Wu, B. Wang, S. Liang, H. Wang, *Angew. Chem., Int. Ed.* **2020**, *59*, 7797.
- [14] X.-Q. Zhang, X.-B. Cheng, X. Chen, C. Yan, Q. Zhang, *Adv. Funct. Mater.* **2017**, *27*, 1605989.
- [15] B. Wen, Z. Deng, P.-C. Tsai, Z. W. Lebens-Higgins, L. F. J. Piper, S. P. Ong, Y.-M. Chiang, *Nat. Energy* **2020**, *3*, 2989.
- [16] S. Cui, P. Zhai, W. Yang, Y. Wei, J. Xiao, L. Deng, Y. Gong, *Small* **2020**, *16*, 1905620.
- [17] Y. Ma, *Energy Environ. Mater.* **2018**, *1*, 148.
- [18] T. J. H. Viugt, K. Malek, B. Smit, *Computational Methods in Catalysis and Materials Science: An Introduction for Scientists and Engineers*, Wiley, Hoboken, NJ **2009**, p. 123.
- [19] Y. Zhao, Z. Zhang, W. Feng, *Toxicology of Nanomaterials*, Wiley, Hoboken, NJ **2016**, p. 333.
- [20] R. Iftimie, P. Minary, M. E. Tuckerman, *Proc. Natl. Acad. Sci. USA* **2005**, *102*, 6654.
- [21] E. Paquet, H. L. Viktor, *Adv. Chem.* **2018**, *2018*, 9839641.
- [22] A. Chakraborty, S. Kunnikuruvan, M. Dixit, D. T. Major, *Isr. J. Chem.* **2020**, *60*, 1.
- [23] J. A. Dawson, T. S. Attari, H. Chen, S. P. Emge, K. E. Johnston, M. S. Islam, *Energy Environ. Sci.* **2018**, *11*, 2993.
- [24] M. Salanne, *Phys. Chem. Chem. Phys.* **2015**, *17*, 14270.
- [25] F. Gschwind, H. Euchner, G. Rodriguez-Garcia, *Eur. J. Inorg. Chem.* **2017**, *2017*, 2784.
- [26] N. Kumar, J. M. Seminario, *J. Phys. Chem. C* **2016**, *120*, 16322.
- [27] R. E. Boyett, M. G. Ford, P. A. Cox, *Solid State Ionics* **1995**, *81*, 61.
- [28] C. L. Ting, M. J. Stevens, A. L. Frischknecht, *Macromolecules* **2015**, *48*, 809.
- [29] S. Lee, J. Jung, Y. Han, *Chem. Phys. Lett.* **2005**, *406*, 332.
- [30] M. I. Chaudhari, J. R. Nair, L. R. Pratt, F. A. Soto, P. B. Balbuena, S. B. Rempe, *J. Chem. Theory Comput.* **2016**, *12*, 5709.

- [31] J. Lim, K.-K. Lee, C. Liang, K.-H. Park, M. Kim, K. Kwak, M. Cho, *J. Phys. Chem. B* **2019**, *123*, 6651.
- [32] J. Hou, M. Yang, D. Wang, J. Zhang, *Adv. Energy Mater.* **2020**, *10*, 1904152.
- [33] M. T. Ong, O. Verners, E. W. Draeger, A. C. T. van Duin, V. Lordi, J. E. Pask, *J. Phys. Chem. B* **2015**, *119*, 1535.
- [34] V. Chaban, *Chem. Phys. Lett.* **2015**, *631–632*, 1.
- [35] J. Barthel, H.-J. Gores, R. Neueder, A. Schmid, *Pure Appl. Chem.* **1999**, *71*, 1705.
- [36] E. Jónsson, P. Johansson, *Phys. Chem. Chem. Phys.* **2012**, *14*, 10774.
- [37] Y. Yamada, K. Furukawa, K. Sodeyama, K. Kikuchi, M. Yaegashi, Y. Tateyama, A. Yamada, *J. Am. Chem. Soc.* **2014**, *136*, 5039.
- [38] L. E. Camacho-Forero, T. W. Smith, P. B. Balbuena, *J. Phys. Chem. C* **2017**, *121*, 182.
- [39] K. Sodeyama, Y. Yamada, K. Aikawa, A. Yamada, Y. Tateyama, *J. Phys. Chem. C* **2014**, *118*, 14091.
- [40] H. Yildirim, J. B. Haskins, C. W. Bauschlicher, J. W. Lawson, *J. Phys. Chem. C* **2017**, *121*, 28214.
- [41] C. Yan, Y.-X. Yao, X. Chen, X.-B. Cheng, X.-Q. Zhang, J.-Q. Huang, Q. Zhang, *Angew. Chem.* **2018**, *130*, 14251.
- [42] S. Bai, Y. Sun, J. Yi, Y. He, Y. Qiao, H. Zhou, *Joule* **2018**, *2*, 2117.
- [43] Z. Li, O. Borodin, G. D. Smith, D. Bedrov, *J. Phys. Chem. B* **2015**, *119*, 3085.
- [44] J. Zhou, H. Ji, J. Liu, T. Qian, C. Yan, *Energy Storage Mater.* **2019**, *22*, 256.
- [45] C. Luo, T. Shen, H. Ji, D. Huang, J. Liu, B. Ke, Y. Wu, Y. Chen, C. Yan, *Small* **2020**, *16*, 1906208.
- [46] H. Li, X. Shen, H. Hua, J. Gao, Z. Wen, X. Wang, L. Peng, D. Wu, P. Zhang, J. Zhao, *Solid State Ionics* **2020**, *347*, 115246.
- [47] L. Li, M. Wang, J. Wang, F. Ye, S. Wang, Y. Xu, J. Liu, G. Xu, Y. Zhang, Y. Zhang, C. Yan, N. V. Medhekar, M. Liu, Y. Zhang, *J. Mater. Chem. A* **2020**, *8*, 8033.
- [48] D. Lin, Y. Liu, Y. Cui, *Nat. Nanotechnol.* **2017**, *12*, 194.
- [49] B. Sun, J. Mindemark, E. V. Morozov, L. T. Costa, M. Bergman, P. Johansson, Y. Fang, I. Furró, D. Brandell, *Phys. Chem. Chem. Phys.* **2016**, *18*, 9504.
- [50] O. Borodin, G. D. Smith, *J. Phys. Chem. B* **2000**, *104*, 8017.
- [51] H. Kasemägi, M. Klintonberg, A. Aabloo, J. O. Thomas, *J. Mater. Chem.* **2001**, *11*, 3191.
- [52] J. Karo, D. Brandell, *Solid State Ionics* **2009**, *180*, 1272.
- [53] D. Brandell, H. Kasemägi, T. Tamm, A. Aabloo, *Solid State Ionics* **2014**, *262*, 769.
- [54] S. Xue, Y. Liu, Y. Li, D. Teeters, D. W. Crunkleton, S. Wang, *Electrochim. Acta* **2017**, *235*, 122.
- [55] K. Lu, J. K. Maranas, S. T. Milner, *Soft Matter* **2016**, *12*, 3943.
- [56] O. Borodin, G. D. Smith, *Macromolecules* **2006**, *39*, 1620.
- [57] D. Brandell, A. Liivat, H. Kasemägi, A. Aabloo, J. O. Thomas, *J. Mater. Chem.* **2005**, *15*, 1422.
- [58] J. Qin, J. J. de Pablo, *Macromolecules* **2016**, *49*, 3630.
- [59] S. P. Ong, Y. Mo, W. D. Richards, L. Miara, H. S. Lee, G. Ceder, *Energy Environ. Sci.* **2013**, *6*, 148.
- [60] L. J. Miara, N. Suzuki, W. D. Richards, Y. Wang, J. C. Kim, G. Ceder, *J. Mater. Chem. A* **2015**, *3*, 20338.
- [61] T. Cheng, B. V. Merinov, S. Morozov, W. A. Goddard, *ACS Energy Lett.* **2017**, *2*, 1454.
- [62] K. Oh, D. Chang, B. Lee, D.-H. Kim, G. Yoon, I. Park, B. Kim, K. Kang, *Chem. Mater.* **2018**, *30*, 4995.
- [63] Y. Mo, S. P. Ong, G. Ceder, *Chem. Mater.* **2012**, *24*, 15.
- [64] N. J. J. de Klerk, E. van der Maas, M. Wagemaker, *ACS Appl. Energy Mater.* **2018**, *1*, 3230.
- [65] S. Xin, Z. Chang, X. Zhang, Y.-G. Guo, *Natl. Sci. Rev.* **2017**, *4*, 54.
- [66] Y. Liang, C.-Z. Zhao, H. Yuan, Y. Chen, W. Zhang, J.-Q. Huang, D. Yu, Y. Liu, M.-M. Titirici, Y.-L. Chueh, H. Yu, Q. Zhang, *InfoMat* **2019**, *1*, 6.
- [67] E. Paled, *J. Electrochem. Soc.* **1979**, *126*, 2047.
- [68] S. Bertolini, P. B. Balbuena, *J. Phys. Chem. C* **2018**, *122*, 10783.
- [69] Y. Zhou, M. Su, X. Yu, Y. Zhang, J.-G. Wang, X. Ren, R. Cao, W. Xu, D. R. Baer, Y. Du, O. Borodin, Y. Wang, X.-L. Wang, K. Xu, Z. Xu, C. Wang, Z. Zhu, *Nat. Nanotechnol.* **2020**, *15*, 224.
- [70] X.-B. Cheng, R. Zhang, C.-Z. Zhao, F. Wei, J.-G. Zhang, Q. Zhang, *Adv. Sci.* **2016**, *3*, 1500213.
- [71] Doron Aurbach, Yair Ein-Eli, Boris Markovsky, Arie Zaban, S. Luski, Y. Carmeli, H. Yamin, *J. Electrochem. Soc.* **1995**, *142*, 2882.
- [72] A. Budi, A. Basile, G. Opletal, A. F. Hollenkamp, A. S. Best, R. J. Rees, A. I. Bhatt, A. P. O'Mullane, S. P. Russo, *J. Phys. Chem. C* **2012**, *116*, 19789.
- [73] K. Tasaki, *J. Phys. Chem. B* **2005**, *109*, 2920.
- [74] B. V. Merinov, S. Naserifar, S. V. Zybin, S. Morozov, W. A. Goddard, J. Lee, J. H. Lee, H. E. Han, Y. C. Choi, S. H. Kim, *J. Phys. Chem.* **2020**, *152*, 31101.
- [75] D. Bedrov, O. Borodin, J. B. Hooper, *J. Phys. Chem. C* **2017**, *121*, 16098.
- [76] T. Ikeshoji, Y. Ando, M. Otani, E. Tsuchida, S. Takagi, M. Matsuo, S.-i. Orimo, *Appl. Phys. Lett.* **2013**, *103*, 133903.
- [77] Z. Yu, D. G. Mackanic, W. Michaels, M. Lee, A. Pei, D. Feng, Q. Zhang, Y. Tsao, C. V. Amanchukwu, X. Yan, H. Wang, S. Chen, K. Liu, J. Kang, J. Qin, Y. Cui, Z. Bao, *Joule* **2019**, *3*, 2761.
- [78] A. Kizilaslan, H. Akbulut, *ChemPlusChem* **2019**, *84*, 183.
- [79] J. Chai, B. Chen, F. Xian, P. Wang, H. Du, J. Zhang, Z. Liu, H. Zhang, S. Dong, X. Zhou, G. Cui, *Small* **2018**, *14*, 1802244.
- [80] X.-R. Chen, Y.-X. Yao, C. Yan, R. Zhang, X.-B. Cheng, Q. Zhang, *Angew. Chem.* **2020**, *132*, 7817.
- [81] A. Aryanfar, D. J. Brooks, A. J. Colussi, B. V. Merinov, W. A. Goddard, M. R. Hoffmann, *Phys. Chem. Chem. Phys.* **2015**, *17*, 8000.
- [82] A. Aryanfar, T. Cheng, A. J. Colussi, B. V. Merinov, W. A. Goddard, M. R. Hoffmann, *J. Phys. Chem.* **2015**, *143*, 134701.
- [83] L. A. Selis, J. M. Seminario, *RSC Adv.* **2018**, *8*, 5255.
- [84] L. Li, S. Basu, Y. Wang, Z. Chen, P. Hundekar, B. Wang, J. Shi, Y. Shi, S. Narayanan, N. Koratkar, *Science* **2018**, *359*, 1513.
- [85] R. Zhang, X.-R. Chen, X. Chen, X.-B. Cheng, X.-Q. Zhang, C. Yan, Q. Zhang, *Angew. Chem., Int. Ed.* **2017**, *56*, 7764.
- [86] L. Fan, S. Li, L. Liu, W. Zhang, L. Gao, Y. Fu, F. Chen, J. Li, H. L. Zhuang, Y. Lu, *Adv. Energy Mater.* **2018**, *8*, 1802350.
- [87] X. Shen, H. Ji, J. Liu, J. Zhou, C. Yan, T. Qian, *Energy Storage Mater.* **2020**, *24*, 426.
- [88] C. Yan, X.-B. Cheng, Y. Tian, X. Chen, X.-Q. Zhang, W.-J. Li, J.-Q. Huang, Q. Zhang, *Adv. Mater.* **2018**, *30*, 1707629.
- [89] M. S. Park, S. B. Ma, D. J. Lee, D. Im, S.-G. Doo, O. Yamamoto, *Sci. Rep.* **2014**, *4*, 3815.
- [90] Y. Sun, J. Zhou, H. Ji, J. Liu, T. Qian, C. Yan, *ACS Appl. Mater. Interfaces* **2019**, *11*, 32008.
- [91] L. Chen, X. Fan, X. Ji, J. Chen, S. Hou, C. Wang, *Joule* **2019**, *3*, 732.



**Yawen Sun** received her Bachelor's degree at Soochow University (2018), China. She is a Master degree candidate at Soochow University with the Grand Prize of Academic Scholarship. Her research interests focus on the high performance electrolyte for lithium-sulfur battery.



**Tingzhou Yang** received his Master's Degree from Soochow University (2017), China. He is currently a Ph.D. student at Institut National de la Recherche Scientifique (INRS, Canada) with a doctoral research scholarship from the Fonds de recherche du Québec-Nature et technologies. His research interests focus on ionic and nanostructured materials for chemical energy conversion and storage.



**Haoqing Ji** is a postdoctoral fellow in College of Energy, Soochow University. He received his Ph.D. degree from Tsinghua University (2018) and Bachelor's degree from Xi'an Jiaotong University (2012). His research interests focus on the theoretical calculations in the field of electrocatalysis and electrochemical energy storage and conversion.



**Tao Qian** is associate professor at Soochow University, Suzhou, China. He received his Ph.D. degree from Nanjing University, China. He is the first batch of outstanding young scholars selected by Soochow University and presides over four scientific research projects including the National Natural Science Foundation of China. His research interests focus on the polymer materials in energy storage and conversion systems.



**Chenglin Yan** is Professor and Dean of the College of Energy at Soochow University in Suzhou, China. He received his Ph.D. from Dalian University of Technology in 2008. In 2011, he became a staff scientist and a group leader at the Institute for Integrative Nanoscience at the Leibniz Institute in Dresden (Germany). His primary research interests focus on electrochemical energy storage.